

# Transport of methanol in poly(methyl methacrylate)

Noreen Thomas and A. H. Windle

*Department of Metallurgy and Materials Science, University of Cambridge, Pembroke Street, Cambridge, UK*

*(Received 23 August 1977)*

The transport kinetics of liquid methanol in PMMA sheet (Perspex) have been studied over the temperature range 23° to 63°C. At the lower temperatures the transport is typical Case II; the methanol penetrating the polymer behind a sharp front which moves at constant velocity. For higher temperatures the concentration of methanol at the front and the front velocity both decrease with increasing penetration. These factors, which are no doubt related, combine to give mass absorption kinetics in which the exponent of time is no longer unity (Case II) but approaches 0.5, the value typical of Fickian diffusion. Iodine has been added to the methanol to make the positions of the penetration fronts readily visible. The iodine does not affect either the rate of penetration or the equilibrium absorption. Measurements of colour density profiles on thin cross-sections using a microdensitometer give a reliable indication of the true methanol profile. The rate at which the methanol penetrates the glassy polymer is proportional to its concentration at the advancing fronts. The apparent activation energy for methanol penetration for constant concentration at the fronts is 25 kcal/mol.

## INTRODUCTION

Solvent diffusion in rubbery polymers can generally be described by Fick's laws of diffusion. Glassy polymers, however, because of their time-dependent responses exhibit 'non-Fickian' or 'anomalous' diffusion kinetics<sup>1</sup>. Hence deviations from Fickian behaviour can occur because of the finite rate at which the polymer structure rearranges itself to accommodate penetrant molecules.

Alfrey *et al.*<sup>2</sup> have categorized diffusion behaviour according to the relative rates of penetrant mobility and the appropriate polymer segment relaxations\* as follows.

(i) Case I (Fickian) – penetrant mobility is much less than segmental relaxation rates.

(ii) Anomalous – penetrant mobility and polymer segment relaxation rates are comparable.

(iii) Case II – penetrant mobility is much greater than segmental relaxation rates. This type of transport is characterized by a sharp boundary separating the inner glassy core from the outer swollen layer and the boundary advances with constant velocity.

Case I (Fickian) and Case II can be viewed as the two limiting types of transport process, with 'anomalous' behaviour lying between them. The amount of penetrant absorbed per unit area at time  $t$  is often represented by:

$$M_t = Kt^n$$

where  $K$  and  $n$  are constants. For Fickian systems  $n = \frac{1}{2}$ , for Case II transport  $n = 1$  and for 'anomalous' diffusion  $\frac{1}{2} < n < 1$ . Case II transport has now been studied in a variety of systems<sup>3-6</sup>.

\* The phrase 'segmental relaxation' is seen as referring to the molecular mechanisms which are the basis of the deviatoric strains associated with Case II transport.

The type of diffusional behaviour observed for any polymer-penetrant system will vary with temperature and penetrant activity. Indeed, over a sufficiently wide range of temperature and/or penetrant activity, a given system should exhibit all the types of behaviour mentioned above<sup>7</sup>.

In this paper we shall present a detailed study of the transport of liquid methanol in sheet PMMA from ambient temperatures to the boiling point of the penetrant and show how the transport behaviour changes from being creep controlled (Case II) at the lowest temperature to approaching Fickian behaviour at the highest temperature. As well as determining the weight gain kinetics of the system, we have used iodine dissolved in the methanol as a marker to measure penetration of the advancing front and the concentration profile across the swollen region. We shall also show that specimen dimensions have an important effect on the apparent transport kinetics.

## EXPERIMENTAL

### *Materials and specimen preparation*

Sheet specimens were cut from 1 and 3 mm thick PMMA (ICI Perspex, molecular weight  $4 \times 10^6$ ,  $T_g$  110°C). Prior to immersion in methanol the specimens were annealed for 1 h at 130°C and oven-cooled to relieve residual stresses. This heat treatment caused a 3% thickness increase with a corresponding reduction in specimen area. It also led to a decrease in molecular weight but this was small compared with the normal limits accepted for Perspex. The water content of the as-received material was found to be 0.8% w/w and this was removed during heat treatment.

### *Procedure for weight gain experiments*

Prewighed specimens were suspended in a methanol bath maintained at the appropriate temperature. After suc-

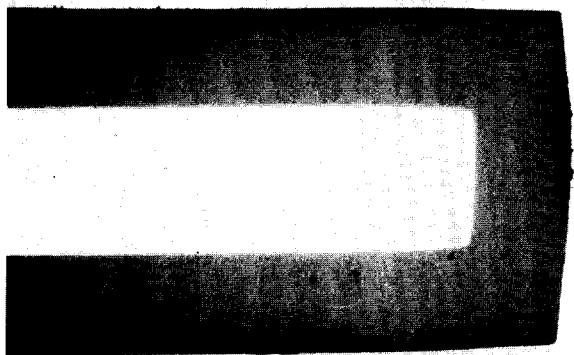


Figure 1 Part of a microtomed cross-section of a PMMA (1 mm) sheet specimen swollen in methanol coloured with iodine. The front is clearly visible. (Note—although the edge of the sheet specimen is shown, all penetration measurements were taken in the central regions of the sheets. Also the dark lines at the specimen surfaces are an optical effect which was eliminated for concentration profile measurements by immersing the specimen in an inert oil of suitable refractive index)

cessive times, specimens were removed from the bath and weighed in stoppered bottles. A different specimen was used for each point on the weight gain graphs to minimize errors due to solvent evaporation, and the data normalized to account for variations in specimen thickness.

All specimens used for weight gain experiments were prepared with dimensions of 40 × 20 × 1 mm. These dimensions were chosen in order to maximize the major surface area with respect to the thickness (as far as was conveniently possible) and hence make the geometry approximate to that of an infinite sheet (see below).

#### Measurement of penetration

As is often the case with diffusion in glassy polymers<sup>1</sup>, a sharp front was seen to separate the swollen and unpenetrated regions. In order to aid observation of this front as it penetrated the material, the methanol was coloured by small additions of iodine. Iodine dissolves in methanol to give a charge transfer complex with a characteristic brown colour and this provides enough contrast to make the advancing front readily visible (Figure 1). Front penetration measurements were made on sections about 60 μm thick cut on a base-sledge microtome. A different specimen was used for each successive measurement and the microtomed section was taken from the centre of the specimen to avoid the effects of accelerated penetration at higher temperatures which occurred near to the specimen edges just before the fronts met.

#### Measurement of iodine-methanol concentration profiles

Iodine concentration profiles were measured on thin sections using a microdensitometer. Microtomed sections about 60 μm thick were cut from specimens immediately on removal from the methanol-iodine bath. Small 'crazes' introduced into the samples on cutting obscured the detail on the microdensitometer traces and so sections were immersed in Nujol oil, which has a refractive index of 1.48 i.e. similar to that of PMMA. The oil rendered the glassy core totally transparent, presumably by filling the 'crazes', and removed the 'noise' from the microdensitometer traces.

## TRANSPORT PARAMETERS

### Weight gain

Weight gain data are presented as increase in weight per unit area of the unswollen specimens. The initial area was calculated from measurements of mass and average thickness using the relationship:

$$\text{Area} = \frac{\text{Mass}}{\text{Density} \times \text{Thickness}}$$

### Effect of variations in sample thickness

1 mm Perspex was found to vary in thickness by up to 10% over the area of a single sheet and by larger amounts between different sheets. This variation presents a problem in that the penetrating front moves into the polymer at a rate independent of specimen thickness, and any attempt to express weight increase as a percentage of original weight will simply imprint the data with the scatter due to the thickness variations between the many specimens used to determine each curve.

However, the expression of weight increase in absolute terms has the disadvantage that the methanol fronts will meet and hence the weight plots level off at different times for specimens of different thickness. Reduction of scatter in the initial part of the plot can therefore only be gained at the expense of increased scatter after the point where the fronts meet.

In this paper the weight increase is expressed in absolute terms in order to minimize the scatter over the initial part of the graph.

### Edge effects

It is clear that in any finite sheet specimen, diffusion occurs through the edges as well as the specimen faces and that this process will result in deviations from the relationship between weight gain and penetration which would characterize an infinite sheet.

In this study the sheet specimens used were 40 × 20 × 1 mm (which corresponds to a value of 0.075 for the ratio of 'edge' area to plane surface area). Since the 'edge effect' imposes curvature on an otherwise linear weight gain plot, it is important to calculate whether this is significant for the specimens used.

The calculation applies to ideal Case II transport where a step concentration profile moves into the specimen at constant rate.

The specimen considered is a rectangular sheet with initial major surface dimensions 'a' and 'b' and thickness 'c'. When the front has penetrated a distance 'd' into the specimen from the original positions of each of the planar and edge faces, the volume  $V_p$  of glassy polymer which has been subsequently swollen is given by:

$$V_p = abc - (a - 2d)(b - 2d)(c - 2d)$$

where the second term represents the volume of the glassy core after each of its dimensions has been reduced by 2d by the advancing fronts.

If  $W_v$  is the increase in weight when a unit volume of glassy polymer has been penetrated, then the total increase in weight after the fronts have penetrated a distance 'd' will be:

$$W = W_v \times V_p$$

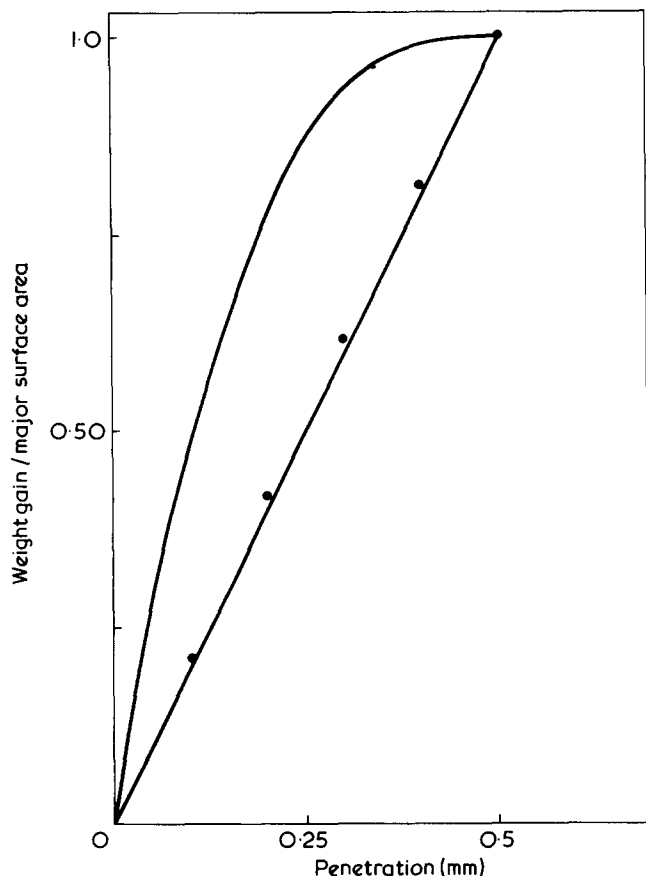


Figure 2 Calculated plots of weight gain/major surface area against penetration distance for a model of ideal Case II transport. —, represent the limiting specimen geometries of a cube and an infinite sheet; ●, sheets 40 mm X 20 mm X 1 mm—the dimensions used in our experiments

and the increase in weight per unit area of the major surface ( $ab$ ) is given by:

$$W_A = \frac{W}{ab} = W_v \left[ c - \left( 1 - \frac{2d}{a} \right) \left( 1 - \frac{2d}{b} \right) (c - 2d) \right]$$

Figure 2 is a plot of  $W_A$  against the penetration depth ' $d$ '. The relationships for the limiting cases of an infinite sheet (linear) and a cube (curved) are shown by continuous lines. The separate points show the relationship for the specimen dimensions actually used, and it is apparent that the approximation to an infinite sheet is not unreasonable, although we must expect the linear weight increase relationship characteristic of Case II transport to be slightly convex to the time axis.

#### Penetration measurements

Front penetration is represented<sup>4</sup> in 2 ways: (i) by the distance ' $l$ ' from the surface of the swollen polymer to the advancing front, and (ii) by the distance ' $d$ ' from the original position of the specimen surface to the front (Figure 3). ' $d$ ' is computed from a measurement of glassy core thickness and  $d \, d'/dt$  is the rate at which the front is moving into the glassy core. ' $l$ ' is relevant in situations where transport of penetrant up to the front significantly controls the overall kinetics. In addition ' $l$ ' is sensitive to the discontinuous reduction in thickness of the swollen region which has been observed at the point at which the fronts meet<sup>8</sup>.

As in the case of the weight measurements, the penetration data are not expressed as percentages of the original sample thickness, since the scatter in thicknesses of the samples would imprint the penetration/time curves.

The penetration is therefore expressed directly in mm.

## RESULTS AND DISCUSSION

### Room temperature transport

Results of the study of methanol transport in sheet PMMA at 24°C are presented in this section. Transport in 1 mm specimens is characteristic of Case II behaviour, whereas deviations from Case II begin to become apparent in 3 mm sheet.

*Weight gain and volume change (1 mm sheet).* Figure 4a shows weight gain per unit area plotted as a function of time. Absorption increases linearly with time up to the point when the sharp fronts meet, which corresponds to the discontinuity on the plot. It is clear from Figure 4a that there is no further gain in weight after the fronts meet, i.e. specimens reach their equilibrium swelling concentration at this point.

Although the behaviour is typical of Case II transport there are two further features worth noting: firstly the plot shows a very slight curvature which is the result of the 'edge effect' and secondly there is an 'incubation time' before sorption begins i.e. the data appear to give a positive intercept on the time axis. A similar effect has been reported in other studies of Case II transport<sup>6,9</sup>.

The % change in specimen volume is plotted as a function of time in Figure 5, together with the weight gain/volume increase ratio. This ratio is constant, indicating that swelling is proportional to absorption (which is often assumed).

*Iodine/methanol penetration and concentration profiles (1 mm sheet).* Penetration data as represented by both ' $l$ ' and ' $d$ ' is linear with time (Figure 4b). The front therefore penetrates the glassy core at a constant rate, independent of its position from the specimen surface. Under these circumstances, the rate controlling factor must be a segmental

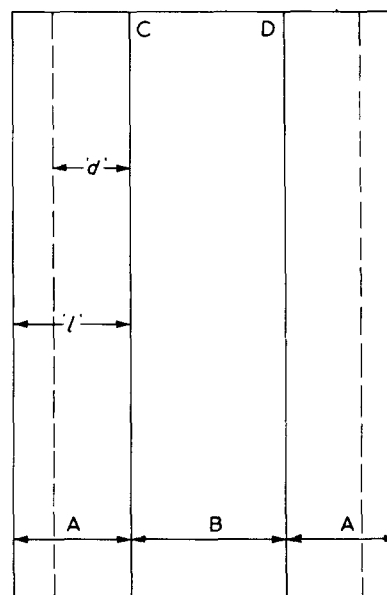


Figure 3 Diagram defining the two front penetration parameters ' $l$ ' and ' $d$ '. A, swollen region; B, glassy region; (---), original position of surfaces; C, D, penetrating fronts

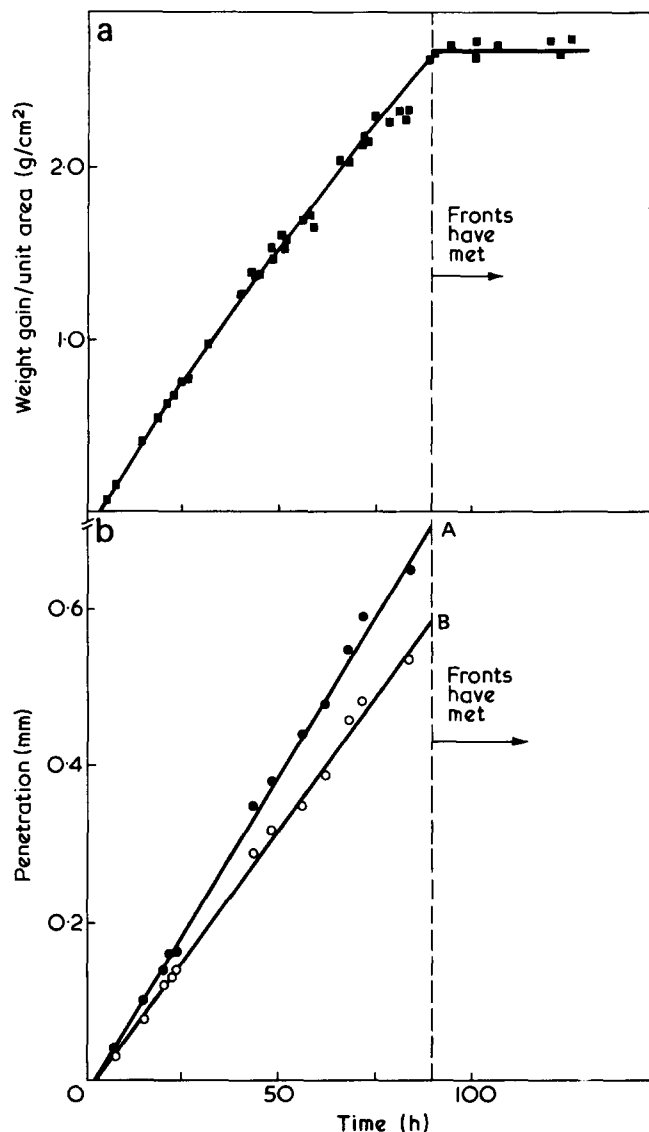


Figure 4 Data at 24°C for 1 mm (nominal) sheet (actual average thickness 1.18 mm). (a) Weight gain/unit area versus time. (b) Penetration as represented by both 'l' (A) and 'd' (B) versus time

'relaxation' process at the front which occurs much more slowly than does diffusion of methanol molecules up to the front. We view this relaxation process in terms of the creeping of polymer segments in response to the deviatoric component of a swelling stress.

A sequence of concentration profiles of methanol stained with iodine from sections of 1 mm sheet specimens are shown in Figures 6a-6c. Specimens were prepared by microtoming and were immersed in oil while the microdensitometer measurements were being taken. These concentration profiles are all of the 'step' type predicted for Case II diffusion<sup>2</sup>. We have found no evidence for the Fickian precursor ahead of the step profile as predicted by Peterlin<sup>10</sup>, although it is possible that the effect exists and is below the limits of detection of our experiments.

*Penetration and concentration profiles (3 mm sheet).*

Penetration data for 3 mm sheet show a deviation from Case II behaviour at long times (Figure 7) i.e. what appears to be ideal Case II transport in a thin specimen becomes anomalous as the front penetrates deeper into the thicker specimen. This behaviour is consistent with the concentration profiles (Figure 8) which are initially 'step' profiles, but show a defi-

nite gradient in the swollen region as the front penetrates deeper into the polymer. These results indicate that for thicker specimens transport is no longer purely 'relaxation' controlled but that the rate of penetration is also affected by diffusion to the front.

*Reliability of iodine as an indicator of front position and methanol concentration gradient.* In the penetration experiments the methanol was made more visible by colouring it with iodine, and it is naturally important to check whether the iodine interferes in any way with the transport kinetics.

Figure 9 shows the weight gain plots for pure methanol and two iodine solutions of different concentration. It is apparent that iodine does not affect the front velocity since the discontinuity representing the point where the fronts meet occurs at the same time in all three cases. Also the shape of all the weight gain plots is characteristic of the step profiles revealed by the iodine.

On microtoming sections from partly swollen specimens, it was possible to detect the front even without iodine since the unpenetrated glassy core crazed and became opaque in cutting. The position of the front revealed in this way was always the same as that observed when iodine was present.

The data of Figure 9 indicate that the iodine/methanol ratio within the polymer is about 5 times that in the surrounding solution. Hence iodine seems to have a greater affinity for PMMA than for methanol, which may be indicative of a specific interaction. However, on the basis of obser-

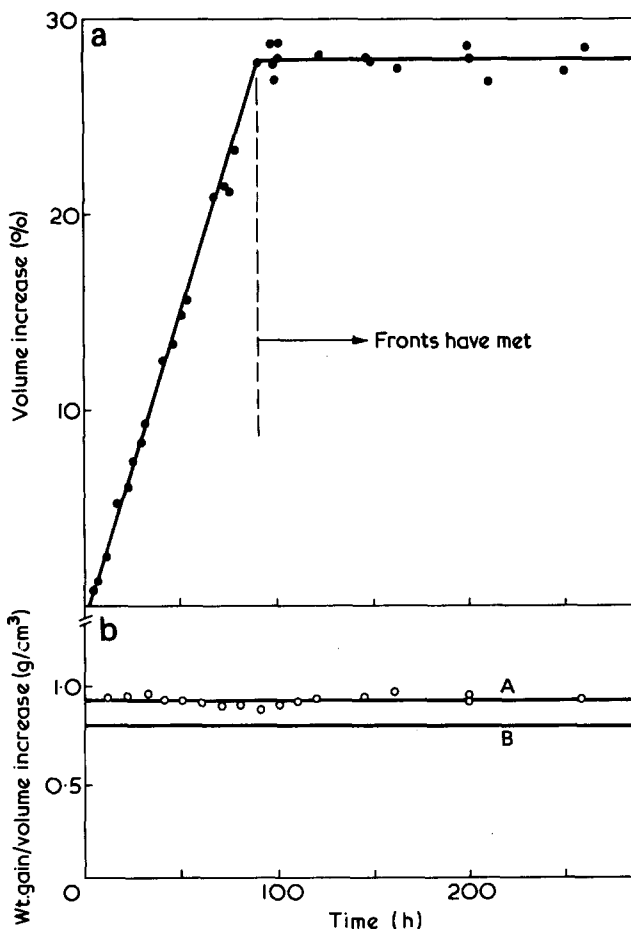


Figure 5 Data at 24°C for 1 mm (nominal) sheet (actual average thickness 1.18 mm). (a) % Volume increase plotted against time. (b) Ratio of weight gain to volume increase versus time (A), compared with density of methanol at 20°C (B)

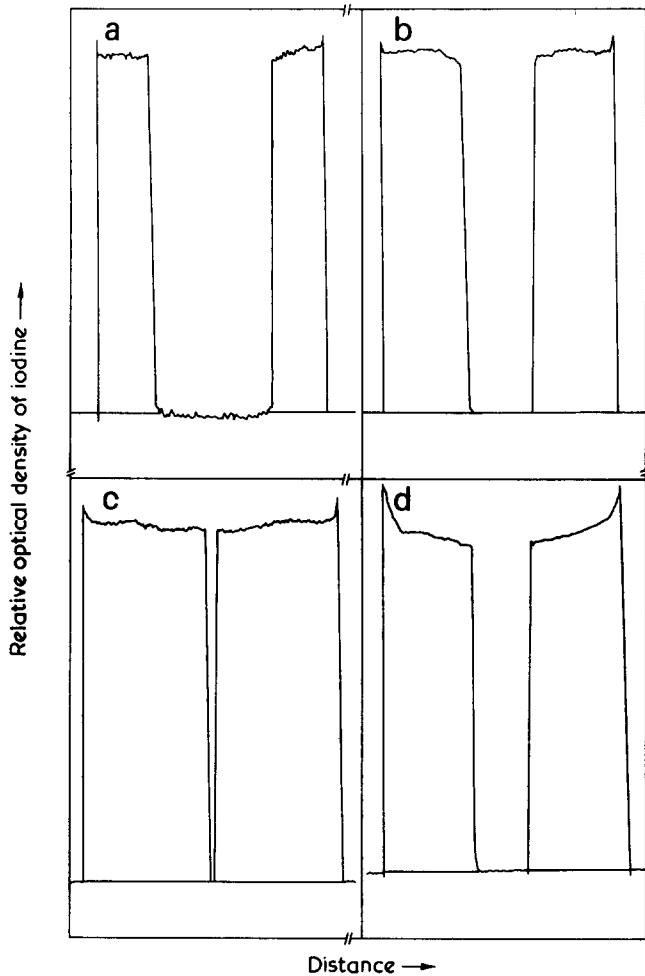


Figure 6 Microdensitometer traces showing concentration profiles across 1 mm (nominal thickness) sheet swollen for given times at 24°C. (Actual average thickness is 1.10 mm). (a), (b), and (c) show sections taken immediately on removal from bath. (d) shows distortion of profile when methanol is allowed to desorb prior to sectioning. (a)  $t = 38$  h; (b)  $t = 60$  h; (c)  $t = 87$  h; (d)  $t = 63$  h at 24°C, 'aged' at 20°C prior to sectioning

variations of changes to the iodine profiles during desorption of methanol, it appears that the iodine does not permanently attach itself to PMMA molecules but remains mobile within the polymer.

Figure 6d shows the concentration profile measured from a specimen which, after removal from the methanol, had been left for 4 days prior to cutting. The distortion near the edge of the profile is thought to be due to methanol and iodine diffusing back to the specimen faces, the methanol evaporating and leaving the observed build up of iodine concentration at the edges of the profile. This may be compared with Figures 6a–6c which show the concentration profiles from sections which were cut immediately on removal of the specimens from the bath. Clearly, the methanol still had to escape, but it must have done so through the planar surfaces of the thin (60  $\mu\text{m}$ ) sections, with the result that any iodine build up on the surfaces will still maintain the original profile.

#### Transport at elevated temperatures

The results presented in this section show that the transport kinetics of methanol in PMMA (1 mm sheet) gradually change from those typical of Case II at ambient temperatures to behaviour approaching 'Fickian' as the temperature is increased up to the boiling point of the solvent (65°C).

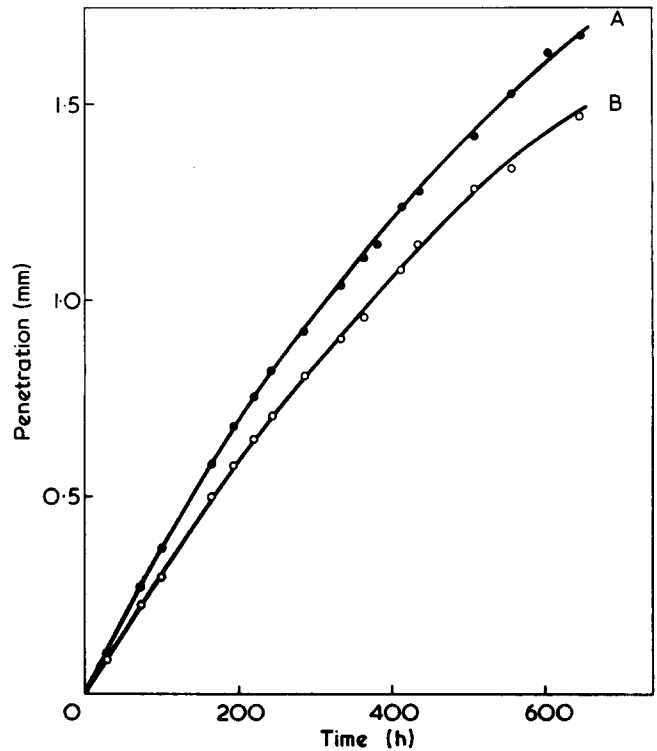


Figure 7 Penetration versus time for 3 mm sheet swollen at 23°C. Deviations from Case II behaviour are apparent. A, 'f' curve; B, 'd' curve

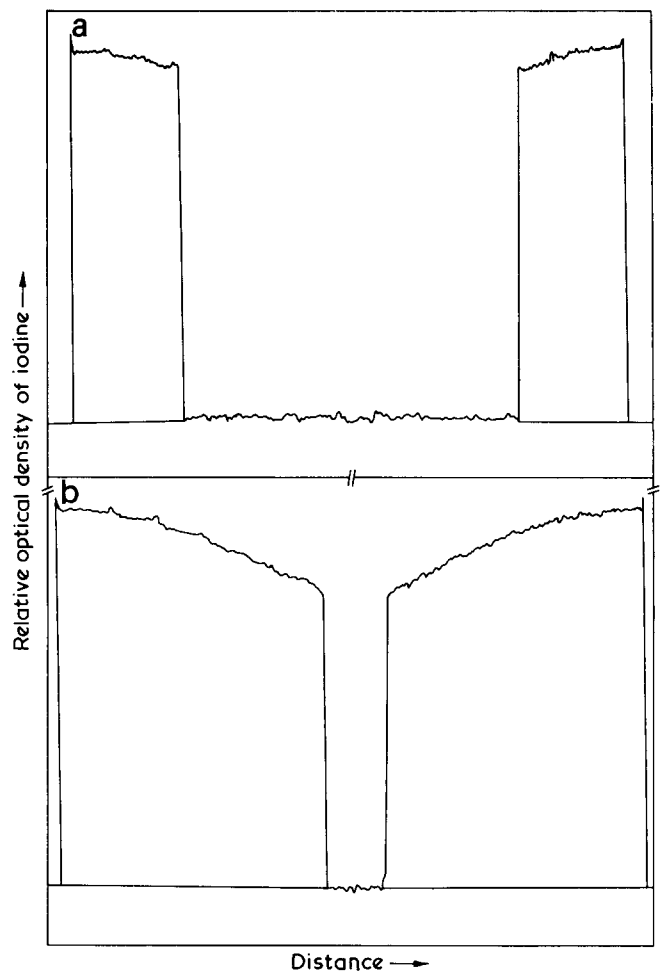


Figure 8 Microdensitometer traces showing concentration profiles across 3 mm sheet specimens swollen for given times at 23°C. (a)  $t = 180$  h; (b)  $t = 550$  h

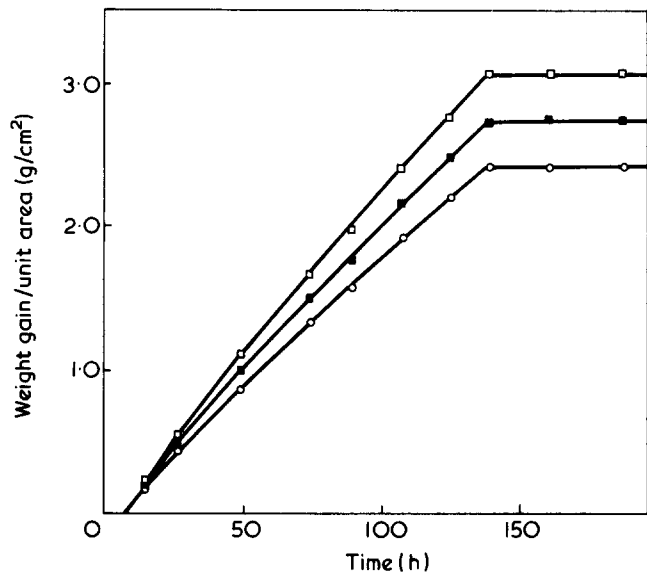


Figure 9 Weight gain/unit area versus time for 1 mm (nominal) sheet specimens swollen at 18°C in methanol and methanol/iodine solutions of different concentrations. The iodine has no effect on the shape of the plots. □, CH<sub>3</sub>OH + I<sub>2</sub>, 40 g/l; ●, CH<sub>3</sub>OH + I<sub>2</sub>, 20 g/l; ○, CH<sub>3</sub>OH

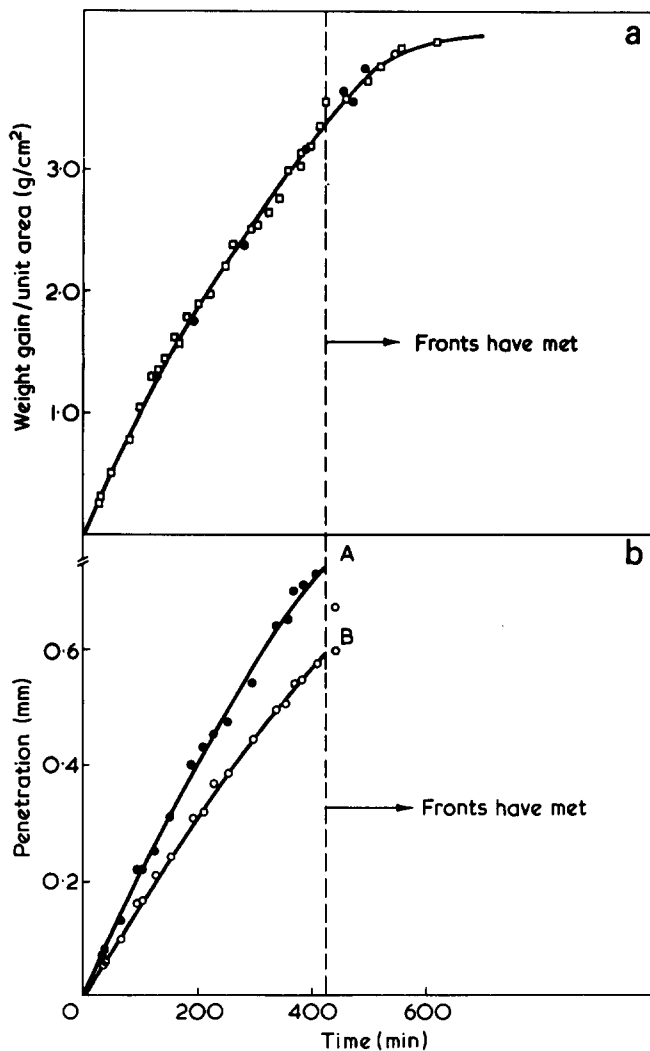


Figure 10 Data for 1 mm (nominal) sheet swollen at 42°C. (Actual average thickness 1.17 mm). (a) Weight gain/unit area versus time, showing experimental points (□) together with values derived from measured concentration profiles (●). (b) Penetration versus time, indicating when fronts meet. A, 'l' curve; B, 'd' curve

Data at 42°C. Figure 10 is a plot of weight gain and front penetration against time. It is clear that the transport kinetics at this temperature deviate from ideal Case II behaviour. The velocity of the fronts is now dependent on their position; a slight deceleration being observed as they penetrate further into the specimen. The weight gain data are also clearly curved and sorption equilibrium is not reached until some time after the fronts have met, supporting the suggestion<sup>11,12</sup> that there is a concentration gradient across the swollen region itself.

A series of four measured concentration profiles corresponding to increasing times of penetration is shown in Figure 11. Sharply defined fronts are apparent as at room temperature but there is now a marked concentration gradient behind them. These profiles represent a situation in which the front velocity, as controlled by relaxation, is more rapid in relation to the diffusivity than it was at room temperature and the gradient is that necessary to 'supply' the advancing front with methanol at a sufficient rate. The fact that the concentration at the fronts at the moment of meeting is less than that at the surfaces (presumed to be the equilibrium value) accounts for the continuation in weight gain after that time until the equilibrium concentration is attained throughout the specimen. From measurements of the area under a series of concentration profiles it is possible to derive the form of the weight gain plot, although it is

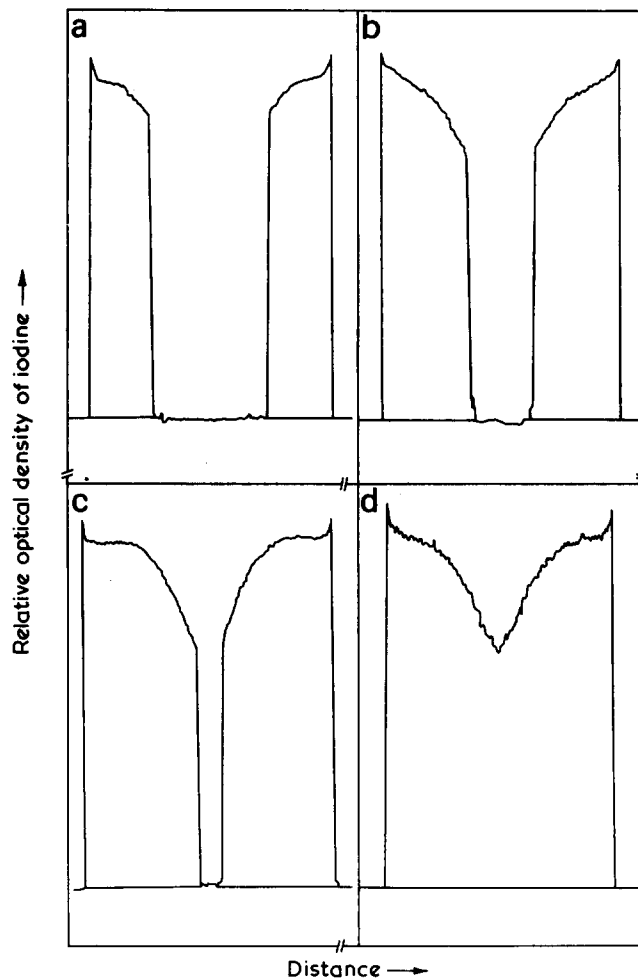


Figure 11 Microdensitometer traces showing concentration profiles across 1 mm (nominal) sheet specimens swollen at 42°C for given times. (Actual average thickness 1.13 mm.) (a)  $t = 196$  min; (b)  $t = 288$  min; (c)  $t = 390$  min; (d)  $t = 458$  min

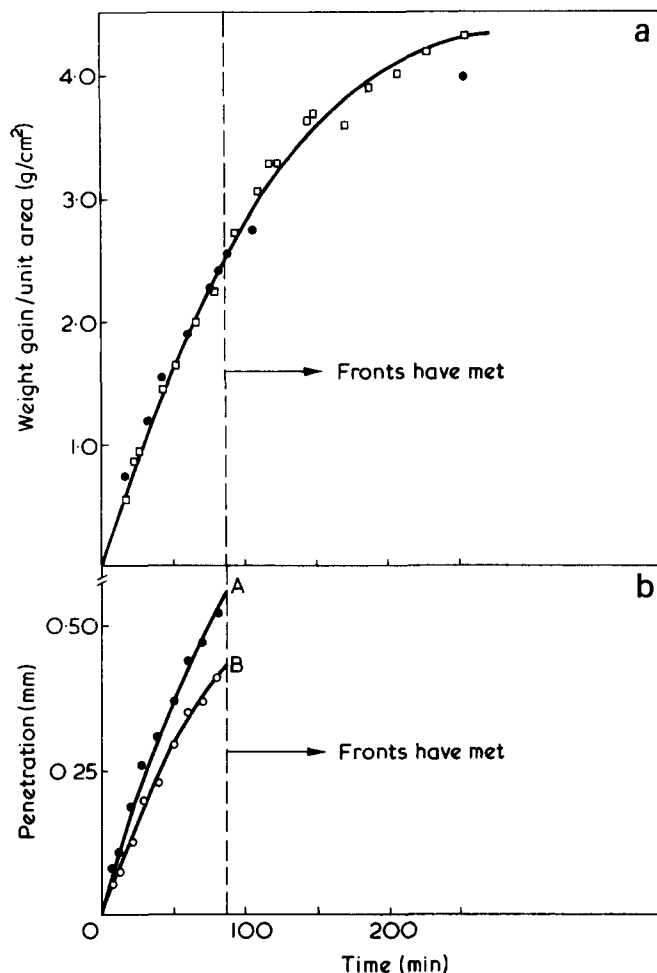


Figure 12 Data for 1 mm (nominal) sheet swollen at 52°C (actual average thickness 0.87 mm). (a) Weight gain/unit area versus time, showing experimental points (□) together with values derived from measured concentration profiles (●). (b) Penetration versus time indicating when fronts meet: A, 'l' curve; B, 'd' curve

necessary to correct for the shape change which occurs on swelling, i.e. the discontinuous increase in area and corresponding decrease in thickness observed when the fronts meet<sup>8</sup>. The plot derived from measurements of the concentration profiles, and suitably normalized, is superimposed on the experimental data in Figure 10a. The good agreement indicates that the iodine concentration profiles closely correspond to those of the methanol.

**Data at 52°C.** The deviations from Case II behaviour described above are better developed at 52°C. The rate of front penetration slows down quite considerably as the fronts become more remote from the specimen surfaces (Figure 12b). In addition the curvature of the weight gain data is more marked and the polymer continues to absorb methanol for a relatively longer period after the fronts have met (Figure 12a).

These effects can be understood in terms of the experimental concentration profiles of Figure 13. Sharply defined fronts still exist between the glassy and swollen regions, with a steep concentration gradient in the swollen polymer. The concentration at the front decreases as penetration proceeds, and this is presumably responsible for the observed decrease in front velocity (Figure 12b). Also the fact that the gradient increases as the methanol concentration decreases towards the front is seen as a qualitative indication of a strong concentration dependence of the diffusion coefficient.

The shape of the weight gain plot has been derived from these profiles; it is superimposed on Figure 12c and the agreement is reasonably good.

As at the lower temperatures, there is still no evidence for any Fickian precursor, although the 'incubation time' seen at room temperature is no longer apparent.

**Data at 62°C.** The data obtained at 62°C represent transport kinetics which approach 'Fickian' behaviour. The weight gain plot of Figure 14a shows that the penetrant fronts meet before the absorption is 60% complete. The penetration data of Figure 14b demonstrate the marked deceleration of the advancing fronts. This behaviour is seen as a consequence of the reducing methanol concentration at the fronts which is commensurate with the steep gradient in the swollen regions. Phenomenologically the penetration process may be described by the relation:

$$d = Kt^n$$

where  $d$  is the penetration,  $K$  is a constant and  $n$  is the exponent of time ( $t$ ).

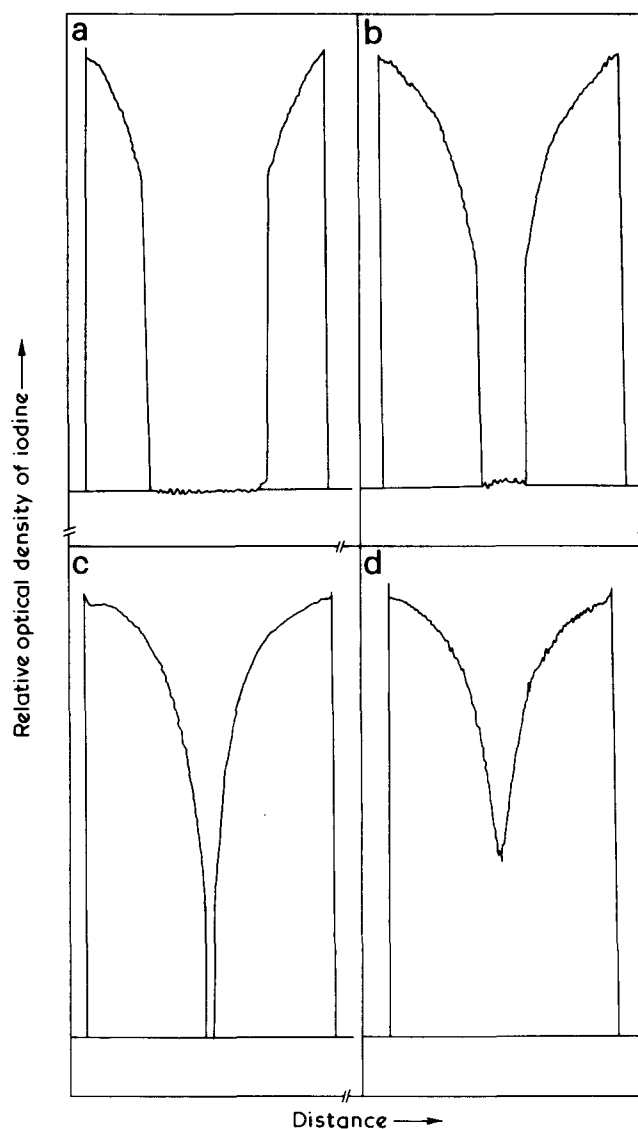


Figure 13 Microdensitometer traces showing concentration profiles across 1 mm (nominal) sheet specimens swollen at 52°C for given times (actual average thickness 1.10 mm). (a)  $t = 32$  min; (b)  $t = 61$  min; (c)  $t = 83$  min; (d)  $t = 90$  min

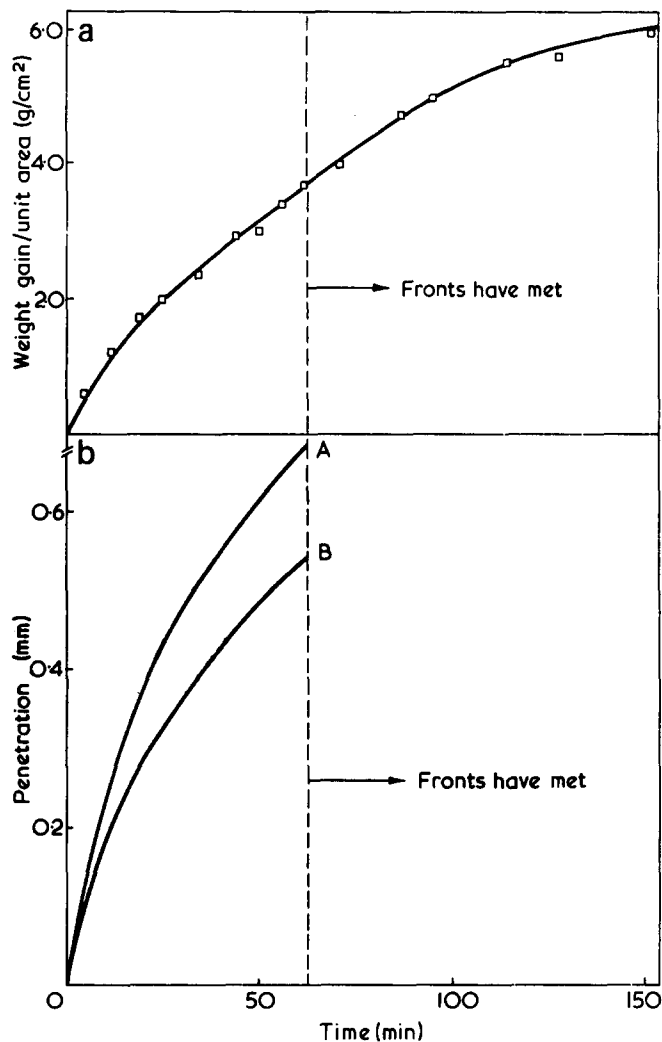


Figure 14 Data for 1 mm (nominal) sheet swollen at 62°C (actual average thickness 1.10 mm). (a) Weight gain/unit area versus time, showing when fronts meet; (b) Penetration versus time. These curves are the mean of data measured at 60° and 64°C. A, 'l' curve; B, 'd' curve

At 62°C the exponent,  $n$ , is 0.65. This is closer to the value of 0.5 typical of a Fickian process than it is to the unit exponent which characterizes Case II transport. It illustrates the extent to which the kinetics of absorption at this temperature are dominated by the diffusion of methanol from the specimen surface to the advancing fronts.

A series of concentration profiles obtained at this temperature is shown in Figures 15a–15c. The concentration gradients behind the fronts are so steep that they tend to merge with the near vertical gradient of the front itself. As at the lower temperatures the area under the profiles has been used to derive the shape of the weight gain plot which is superimposed as the solid round points on the experimental data in Figure 16. (Again corrections were made to take into account the shape change which occurs as the fronts meet, and the surface concentration was assumed to be the equilibrium value.) The agreement is less satisfactory than at lower temperatures and we are faced with the question of whether this is the result of the iodine diffusing less rapidly than the methanol and hence indicating profiles which are different from those of the methanol. Indeed it is to be expected that any tendency of the iodine molecules to lag behind the methanol will be most marked at this high temperature where diffusion in the swollen polymer is such an important factor.

*Behaviour of the iodine solute at 62°C.* As a first step, measurements were made of the influence of different iodine concentrations in the methanol on the weight gain kinetics. These are shown in Figure 17, the experiment being similar to that carried out at 24°C (Figure 9). As at 24°C the shape of the plots is not affected by the iodine; neither is the penetration rate, the fronts meeting after the same time irrespective of iodine concentration. (The time at which the fronts met when methanol alone was used was ascertained from the pronounced increase in specimen area which, at this temperature, occurs at virtually the same instant.)

The comparison between the shapes of the weight plots at different temperatures is not necessarily a particularly sensitive test for parity between iodine and methanol profiles. It is conceivable that an 'iodine lag' sufficient to account for the less than perfect fit of Figure 16 would not detectably change the shape of the weight plot in the case of absorption of methanol/iodine solutions.

In order to resolve this question a series of profile

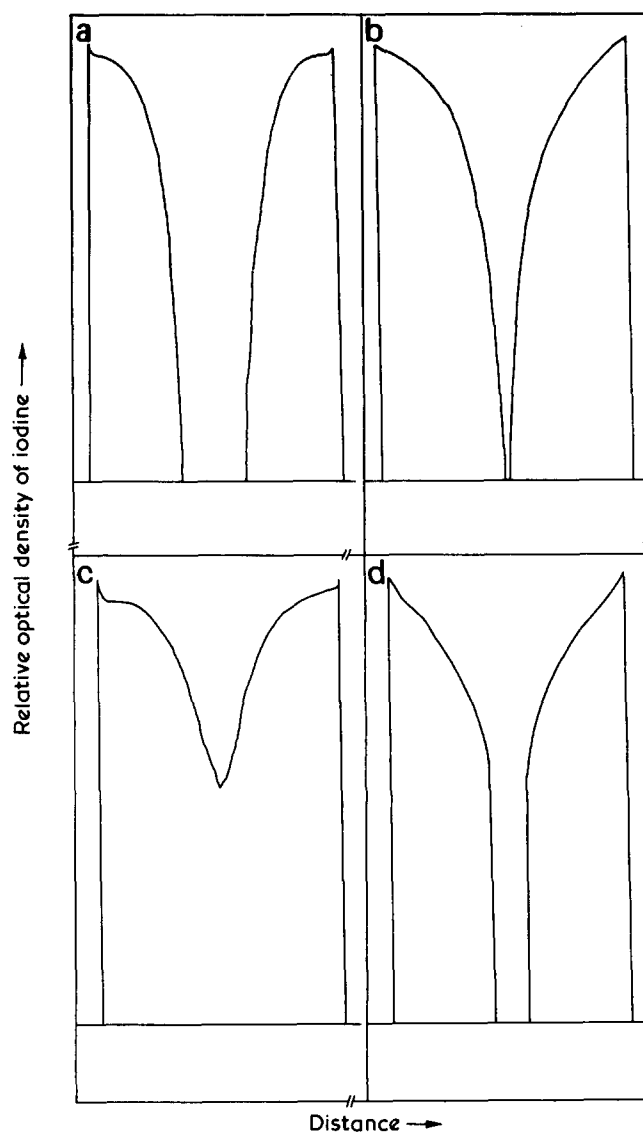


Figure 15 Microdensitometer traces showing concentration profiles across 1 mm (nominal) sheet specimens swollen at 62°C (actual average thickness 1.10 mm). (a)  $t = 30$  min; (b)  $t = 61$  min; (c)  $t = 65$  min. (a), (b) and (c) show sections taken immediately on removal from bath. (d) Shows distortion of profile when specimen is 'aged' at 20°C prior to sectioning,  $t = 45$  min at 62°C



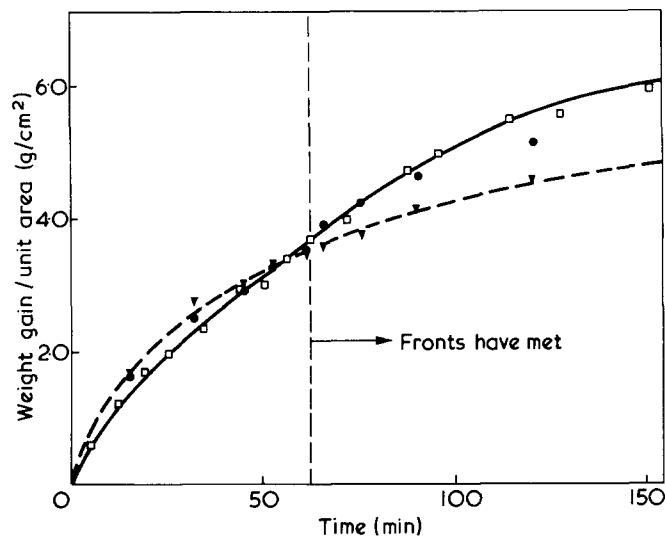


Figure 16 Weight gain/unit area versus time for 1 mm (nominal) sheet (actual average thickness 1.10 mm) swollen at 62°C, showing experimental data, points derived from measured profiles and points derived from 'aged' profiles with 'sharpened' fronts. □, Experimental; ●, derived from measured profiles; ▼, derived from 'aged' profiles with sharpened fronts

measurements were made on specimens which had been swollen at 62°C and then held at 20°C for several hours prior to sectioning. At the lower temperature the front will be effectively frozen but the diffusivity of the iodine and methanol in the swollen regions will not be as drastically reduced. In this way an 'iodine lag' at 62°C would be detectable by a change in profile during the period at 20°C as the iodine (and hence the observed profile) caught up with the true methanol distribution. Figure 15d shows the changed profile. There is a slight build up in iodine concentration at the surface, a phenomenon resulting from the desorption of the methanol and discussed in the previous section. In addition, however, there is a significant increase in iodine concentration at the fronts which are now clearly defined and no longer merge with steep concentration gradients in the swollen material immediately behind them. The position of the fronts does not change appreciably during the 'ageing' period.

There are two possible explanations for this change of profile.

(i) The iodine diffuses more slowly than the methanol at 62°C. The period at 20°C from removal from the methanol until the time when the methanol concentration is significantly lowered by evaporation from the outer surfaces enables the iodine to catch up with the true methanol front. The profile with the sharpened front seen after 'ageing' is thus a better representation of the true methanol distribution during transport at 62°C.

(ii) Parity between methanol and iodine concentrations is maintained at all times. The changes in the observed profile during 'ageing' result from the diffusion of methanol (and iodine) down the especially steep concentration gradients behind the fronts which behave more or less as barriers over the comparatively short period at 20°C. The iodine profile measured immediately after the specimen is removed from the 62°C bath is thus the true representation of the methanol distribution at this temperature.

In order to determine which of these explanations is correct, the shape of the weight gain plot was derived from the profiles in which the fronts had 'sharpened up' during the

'ageing' period at 20°C. These data (▼) are also plotted on Figure 16. The fit with the experimental weight gain plot is much worse than was obtained using the immediate profiles (i.e. those not modified by an 'ageing' period), the deviations previously observed being much magnified.

These observations using the 'aged' samples give some indication why the weight gain plot which had been derived from the 'immediate' profiles did not fit perfectly with the data. It is probable that some degree of profile modification had begun to occur in the period (~5 min) between removal of the sheet specimens from the 62°C bath and the point at which the iodine profile was effectively 'fixed' by desorption of the methanol from the microtomed slice.

We conclude therefore that the second of the two explanations above is the better and that, as far as we can reasonably determine, parity is maintained between the concentrations of methanol and iodine and an observed iodine concentration profile gives an accurate representation of that of the methanol.

#### General review of data

Hitherto the methanol absorption data have been introduced progressively in sections devoted to successively higher temperatures. This presentation has provided a framework for the introduction of substantial amounts of data and also a detailed assessment of the suitability of dissolved iodine as an indicator of methanol concentration.

The purpose of this section is to draw together aspects of the data and submit them to analysis along more or less traditional lines.

Table 1 is a statement of the measurements of equilibrium absorption at various temperatures. The data, expressed in terms of the volume fraction of methanol is very similar indeed to that of Andrews, Levy and Willis<sup>13</sup> which has been subsequently formalized by Hopfenberg, Nicolais and Drioli<sup>6</sup> as a Van't Hoff plot. It is no surprise that our data

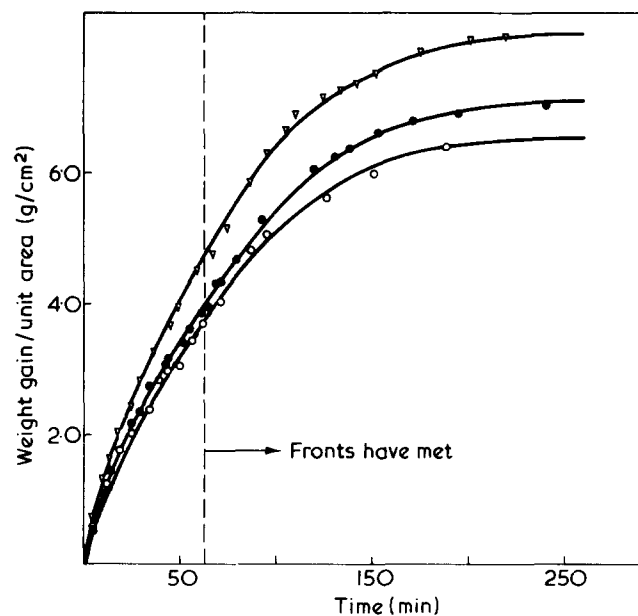


Figure 17 Weight gain/unit area versus time for specimens (1.10 mm) swollen at 62°C in methanol and methanol/iodine solutions of different concentrations. Iodine has no apparent effect on the shape of the plots

Table 1 Equilibrium methanol absorption at various temperatures

Temperature (°C)	Equilibrium (% wt gain)	Volume fraction methanol
24	21	0.24
30	23.5	0.26
38	28	0.29
42	30	0.31
46	35	0.34
52	39	0.37
57	44	0.40
60	48	0.42
62	49	0.42
65	53	0.44

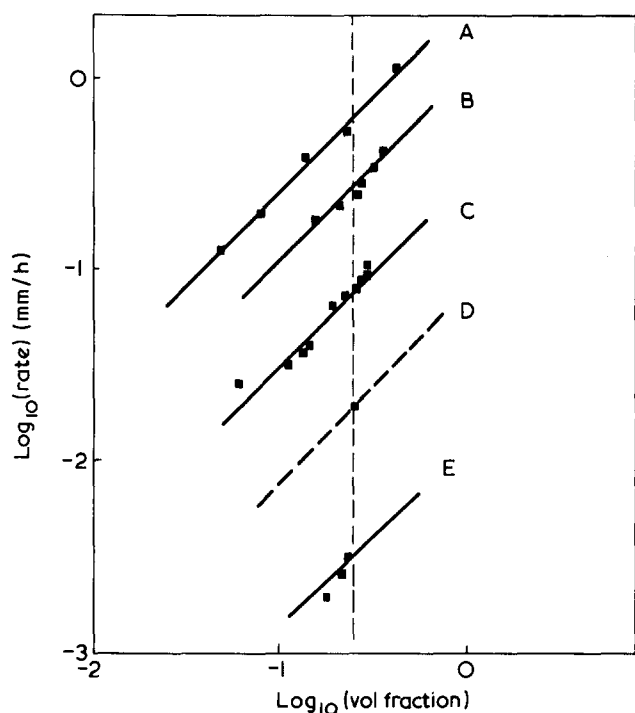


Figure 18 Penetration rate plotted against front concentration in log/log format. The rate of penetration appears to be proportional to the front concentration, in that the data fit fairly well to the straight lines of unit slope. A, 62°C; B, 52°C; C, 42°C; D, 30°C; E, 23°C

yields a value for the heat of mixing ( $\Delta H$ ) of 3.0 kcal/mol which is very close to the Andrews/Hopfenberg value of 2.8 kcal/mol.

The fact that the iodine marker technique makes it possible to measure the methanol concentration actually at the fronts, means that we can relate concentration to penetration rate at various stages during absorption at each temperature. This is particularly relevant at the higher temperatures where both the methanol concentration at the front and the penetration rate significantly decrease as absorption proceeds. Figure 18 shows rate/concentration data presented in log/log format. A straight line isotherm of unit slope is drawn through each data set. The measure of agreement is such that there is no reason for supposing that the relationship between the penetration rate and the concentration at the front is anything but first order. That is, the penetration rate is proportional to methanol concentration at the front.

Two comments regarding the penetration/concentration data at 62°C are appropriate: firstly, it is difficult to assess the precise concentration at the front when this is low (i.e.

at substantial penetrations) and the way in which the two data points of lowest concentration lie on the 45° line must be to some extent fortuitous. Secondly, if the front concentrations used had been those measured *after* the ageing period (see previous section) then the data would lie on a slope of gradient between two and three, quite out of keeping with the general trend. This appears as further evidence that the iodine provides an accurate representation of the methanol concentration.

It is convenient to express the temperature dependence of penetration rate for a constant methanol concentration at the front in terms of the slope of an Arrhenius plot. However in this case it is not possible to identify any single activation process and there is no reason why the plot should be linear. In fact the data are much more likely to obey an equation of WLF form. The Arrhenius plot in Figure 19 is calculated for a methanol concentration at the front of 23.5% w/w (0.26 volume fraction) so as to include the lone datum at 30°C, although the apparent activation energy will be independent of concentration within the data bounds of Figure 18. The value of 25 kcal/mol for the apparent activation energy for Case II transport is within the range of those previously reported for alkane/polystyrene systems<sup>11</sup> but less than those obtained in studies of the transport of higher alcohols in PMMA<sup>12</sup>.

## CONCLUSIONS

- (1) At ambient temperatures the absorption of liquid methanol by PMMA follows Case II kinetics. Both the increase in specimen weight and the penetration of the sharp methanol front are linear with time.
- (2) As the temperature of absorption is increased up to the boiling point of methanol, departures from Case II kinetics become increasingly significant and the exponent of time describing the methanol uptake approaches 0.5 ~ the

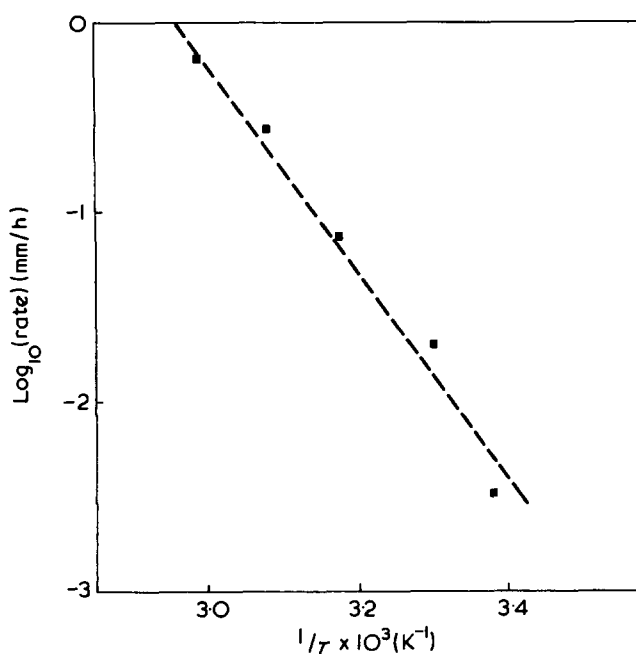


Figure 19 Arrhenius plot showing log rate versus  $1/T$  at a fixed front concentration (volume fraction = 0.26). The points lie on a curve (see text) but an apparent activation energy has been calculated from the mean slope

value typical of Fickian diffusion. The trend towards Fickian behaviour at the higher temperatures can be explained in terms of concentration gradients in the swollen polymer behind the advancing fronts which are observed to steepen as the temperatures is increased.

(3) The dissolution of iodine in the methanol enables the positions of the methanol fronts to be readily observed on cross-sections microtomed from the polymer sheets. The iodine in concentrations of less than 40 g/l has no effect on the rate of methanol absorption.

(4) The colour density due to the iodine in the microtomed cross-sections is a reliable indicator of the methanol concentration for this particular system.

(5) The methanol concentration gradient observed in the swollen polymer behind the penetrant fronts steepens as the concentration decreases. This is seen as a qualitative indication of the marked concentration dependence of the diffusion coefficient of methanol in swollen PMMA.

(6) The rate at which the methanol fronts penetrate the glassy core is proportional to the methanol concentration at the fronts.

(7) The apparent activation energy for front penetration at constant methanol concentration (at the fronts) is 25 kcal/mol.

## APPENDIX

### *A note on the chemistry of iodine solutions*

In this study iodine has been used as a dye to follow the methanol front position and facilitate measurement of concentration profiles. The nature of the methanol/iodine solutions must determine both the success and limitations of our technique and an additional note on their chemistry is appropriate.

Iodine dissolves in organic solvents to give solutions whose colour depends on the nature of the solvent. Solvation and 1:1 complex formation can occur in the case of donor solvents such as alcohols and ketones. The bonding energy between I<sub>2</sub> and the solvent may be attributed to a partial transfer of charge and so the interaction is termed 'charge transfer' complex formation<sup>14,15</sup>. Also the diameter of the I<sub>2</sub> molecule is about 5.5 Å, and this is small compared with most organic dyes, which are usually extensively conjugated chromophores. Hence the advantages of iodine are its specific interaction with the solvent and its relatively small size, both of which favour its ability to diffuse with the solvent.

It should be noted however that bromine rapidly dissolves PMMA, and super-saturated solutions of iodine in methanol were found to cause PMMA to gel and eventually to dissolve.

The solutions used were therefore kept fairly dilute at 30 g/l. Also iodine sublimes at about 60°C, so its use may be limited much above this temperature.

Although iodine has been used successfully as a dye in the methanol/PMMA system, the chemistry of this three component system is certainly complicated. It is not possible to predict that other solvent/iodine/polymer systems will be similarly well behaved, and it will be necessary to test thoroughly the reliability of iodine as an indicator of solvent concentration before it is used with any different polymer/solvent combinations.

## ACKNOWLEDGEMENTS

The authors wish to thank Professor H. B. Hopfenberg who, during a recent period spent at the Department of Chemical Engineering at this University, did much to stimulate the further development of these studies, and Mr E. Zichy of ICI Ltd for his enthusiastic encouragement. We also thank Professor R. W. K. Honeycombe for enabling the work to take place in his Department, and Mr B. Ambrose of the Cavendish Laboratories for assistance with the microdensitometry. N.L.T. acknowledges the support of a Science Research Council studentship.

## REFERENCES

- 1 Park, G. S. 'Diffusion in Polymers', (Eds J. Crank and G. S. Park), Academic Press, London, 1968, Ch. 5
- 2 Alfrey, T., Gurnee, E. F. and Lloyd, W. G. *J. Polym. Sci. (C)* 1966, **12**, 249
- 3 Hopfenberg, H. B., Holley, R. H. and Stannett, V. *Polym. Eng. Sci.* 1969, **9**, 242
- 4 Kwei, T. K. and Zupko, H. M. *J. Polym. Sci. (A-2)* 1969, **7**, 867
- 5 Jacques, C. H. M. and Hopfenberg, H. B. *Polym. Eng. Sci.* 1974, **14**, 449
- 6 Hopfenberg, H. B., Nicolais, L. and Drioli, E. *Polymer* 1976, **17**, 195
- 7 Hopfenberg, H. B. and Frisch, H. L. *J. Polym. Sci. (B)* 1969, **7**, 405
- 8 Thomas, N. L. and Windle, A. H. *Polymer* 1977, **18**, 1195
- 9 Weinberg, D. *J. Membr. Sci.* in press
- 10 Peterlin, A. *Makromol. Chem.* 1969, **124**, 136
- 11 Nicolais, L., Drioli, E., Hopfenberg, H. B. and Tidone, D. *Polymer* 1977, **18**, 1137
- 12 Nicolais, L., Drioli, E., Hopfenberg, H. B. and Caricati, G. *J. Membr. Sci.* in press
- 13 Andrews, E. H., Levy, G. M. and Willis, J. *J. Mater. Sci.* 1973, **8**, 1000
- 14 Andrews, L. J. and Keefer, R. M. *Adv. Inorg. Chem. Radiochem.* 1961, **3**, 91
- 15 Julien, L. M., Bennett, W. E. and Person, W. B. *J. Am. Chem. Soc.* 1969, **91**, 6915